

**Table S1. Antibodies used in Luminex assays**

Protein	Capture Antibody	Detection Antibody	Detection limit, pg/mL
CCL14	R&D Systems # MAB3241	R&D Systems # BAF324	10
DKK3	R&D Systems # DY1118	R&D Systems # DY1118	10
IL1RAP	R&D Systems # DY676	R&D Systems # DY676	40
IL6ST	R&D Systems # MAB628	R&D Systems # BAF228	10
LGALS3BP	R&D Systems # DY2226	R&D Systems # DY2226	40

**Table S2. Proteins associated with sclerotic GVHD**

Gene name	Gene description	Mean fold difference in sclerotic GVHD compared with each group*							
		Experiment in male				Experiment in female			
		No GVHD	cGVHD /w IST	cGVHD /wo IST	BOS	No GVHD	cGVHD /w IST	cGVHD /wo IST	BOS
ACP1	Low molecular weight phosphotyrosine protein phosphatase	0.79	0.44	0.48	0.35	0.55	0.28	0.25	0.33
ADAMTSL4	ADAMTS-like protein 4	2.02	4.95	3.37	3.11	3.33	3.66	2.73	2.11
AGT	Angiotensinogen	0.70	0.49	0.64	0.46	0.61	0.50	0.47	0.59
ALDOB	Fructose-bisphosphate aldolase B	0.69	0.42	0.58	0.45	0.56	0.38	0.31	0.37
ANG	Angiogenin	0.62	0.70	0.49	0.43	0.74	0.61	0.51	0.62
APLP1	Amyloid-like protein 1	2.56	6.75	6.93	3.99	4.71	11.0	1.91	2.17
APOB	Apolipoprotein B-48	1.00	0.65	0.63	0.57	0.78	0.55	0.48	0.54
APOM	Apolipoprotein M	1.03	0.56	0.55	0.49	0.63	0.42	0.38	0.40
BMP1	BMP1 protein	8.55	19.7	20.8	6.74	2.96	2.30	1.57	1.24
C19orf54	UPF0692 protein C19orf54	0.65	0.43	0.45	0.42	0.55	0.32	0.26	0.34
C1QA	Complement C1q subcomponent subunit A	0.72	0.48	0.47	0.42	0.71	0.47	0.47	0.51
C3	Complement C3	0.88	0.44	0.52	0.43	0.67	0.45	0.35	0.41
CADM1	Cell adhesion molecule 1	1.69	3.58	4.79	4.31	2.17	3.01	2.29	2.34
CAST	DNA-directed RNA polymerase I subunit RPA34	1.24	2.44	3.78	3.27	1.24	3.02	4.20	2.91
CCL14	C-C motif chemokine 14	0.70	0.55	0.55	0.41	0.79	0.65	0.64	0.63
CD14	Monocyte differentiation antigen CD14	0.78	0.65	0.55	0.61	0.69	0.61	0.48	0.56
CD163	Scavenger receptor cysteine-rich type 1 protein M130	0.18	0.36	0.14	0.23	0.66	0.49	0.50	0.48
CDH5	Cadherin-5	2.97	6.27	5.52	5.76	1.42	2.93	2.54	2.73
CEP295NL	Protein LOC100653515	0.86	0.50	0.53	0.37	0.73	0.56	0.59	0.60
CFL1	Cofilin-1	1.08	0.52	0.53	0.54	0.67	0.58	0.55	0.51
CHGA	Chromogranin A (Parathyroid secretory protein 1)	2.13	3.66	4.35	4.38	2.11	1.97	2.54	1.80
CRISP3	Cysteine-rich secretory protein 3	0.64	0.56	0.64	0.56	0.71	0.57	0.51	0.42
CSF1R	Macrophage colony-stimulating factor 1 receptor	0.72	0.57	0.56	0.59	0.53	0.30	0.23	0.27
CTSD	Cathepsin D light chain	1.02	0.58	0.57	0.55	0.54	0.32	0.27	0.28
DKK3	Dickkopf-related protein 3	3.60	5.53	5.08	3.84	2.07	4.02	2.18	1.90
DSC1	Desmocollin-1	0.98	0.36	0.55	0.46	0.59	0.38	0.44	0.46
F11	Coagulation factor XI	3.35	6.36	8.37	3.61	2.17	2.94	3.33	2.50
FBLN1	Fibulin-1	0.69	0.54	0.54	0.52	0.74	0.56	0.57	0.58
FGFR1	Fibroblast growth factor receptor 1	5.78	7.35	7.71	12.8	3.90	5.25	1.98	4.30
GAPDH	Glyceraldehyde-3-phosphate dehydrogenase	0.65	0.44	0.56	0.43	0.61	0.49	0.38	0.40
GHR	Growth hormone receptor	1.12	2.89	2.92	6.25	2.16	2.29	1.89	1.99
GLIPR2	Golgi-associated plant pathogenesis-related protein 1	1.23	0.58	0.57	0.60	0.67	0.47	0.36	0.43
GPLD1	Phosphatidylinositol-glycan-specific phospholipase D	0.85	0.50	0.50	0.50	0.72	0.64	0.55	0.57

GSR	Glutathione reductase_ mitochondrial	0.76	0.42	0.47	0.44	0.83	0.52	0.45	0.48
HP	Haptoglobin	0.42	0.47	0.30	0.09	0.99	0.12	0.58	0.45
HSP90B1	Endoplasmic	0.34	0.46	1.11	0.51	0.57	0.49	0.36	0.47
HSPA8	Heat shock cognate 71 kDa protein	0.75	0.41	0.41	0.38	0.64	0.40	0.32	0.37
IL1RAP	Interleukin-1 receptor accessory protein	0.77	0.66	0.62	0.51	0.60	0.39	0.32	0.34
IL6ST	Interleukin-6 receptor subunit beta	1.90	4.09	2.55	3.92	3.12	5.82	3.44	3.15
ISLR	Immunoglobulin superfamily containing leucine-rich repeat protein	0.82	0.48	0.61	0.49	0.59	0.40	0.31	0.35
KRT2	Keratin type II cytoskeletal 2 epidermal	0.78	0.43	0.55	0.44	0.69	0.47	0.54	0.51
KRT6B	Keratin type II cytoskeletal 6B	0.82	0.52	0.58	0.45	0.73	0.60	0.58	0.52
KRT77	Keratin type II cytoskeletal 1b	0.73	0.51	0.60	0.60	0.77	0.49	0.57	0.56
LAMP2	Lysosome-associated membrane glycoprotein 2	0.88	0.51	0.53	0.42	0.54	0.25	0.13	0.20
LCP1	Plastin-2	0.96	0.41	0.56	0.13	0.64	0.47	0.36	0.42
LGALS3BP	Galectin-3-binding protein	1.04	0.55	0.56	0.49	0.57	0.38	0.29	0.32
LTBP1	Latent-transforming growth factor beta-binding protein 1	3.00	6.21	4.81	4.85	1.98	2.57	2.22	2.56
LYZ	Lysozyme C	0.81	0.50	0.53	0.50	0.59	0.38	0.29	0.35
MINPP1	Multiple inositol polyphosphate phosphatase	0.39	0.20	0.48	0.77	0.51	0.21	0.13	0.18
MYL6	Myosin light polypeptide 6	3.74	7.18	6.82	3.94	1.49	2.02	1.84	2.46
MYOC	Myocilin	0.87	0.48	0.55	0.43	0.49	0.25	0.11	0.14
NTRK2	BDNF/NT-3 growth factors receptor	0.68	2.20	4.79	5.15	1.03	1.69	2.49	2.38
ORM2	Alpha-1-acid glycoprotein 2	3.77	3.71	2.51	2.55	2.58	2.37	1.64	1.64
PEPD	Xaa-Pro dipeptidase	0.78	0.46	0.5	0.41	0.77	0.51	0.38	0.42
PI16	Peptidase inhibitor 16	0.80	0.56	0.62	0.57	0.61	0.35	0.35	0.42
PKM	Pyruvate kinase	0.31	0.42	0.52	0.28	0.73	0.50	0.45	0.47
PLS3	Plastin-3	3.02	5.65	3.34	4.17	8.15	8.74	5.58	4.34
PON1	Serum paraoxonase/arylesterase 1	0.62	0.47	0.50	0.45	0.74	0.61	0.50	0.57
POTEF	POTE ankyrin domain family member F	0.71	0.51	0.48	0.66	0.72	0.49	0.40	0.54
PPIA	Peptidyl-prolyl cis-trans isomerase A	0.64	0.45	0.59	0.52	0.61	0.42	0.40	0.46
RAD18	E3 ubiquitin-protein ligase RAD18	3.07	2.48	1.96	2.30	3.19	5.60	2.43	2.25
SERPINA6	Corticosteroid-binding globulin	3.28	5.99	4.38	6.03	3.05	1.73	2.47	2.01
SLURP1	Secreted Ly-6/uPAR-related protein 1	0.94	0.58	0.59	0.38	0.58	0.39	0.35	0.43
SYBU	Syntabulin	0.66	0.51	0.66	0.45	0.58	0.40	0.41	0.46
TPI1	Triosephosphate isomerase	0.98	0.53	0.53	0.46	0.70	0.49	0.48	0.48
TTR	Transthyretin	2.15	2.34	2.64	2.51	3.53	4.82	3.23	1.80
TUBA1C	Tubulin alpha-1C chain	0.68	0.52	0.63	0.39	0.57	0.34	0.28	0.36
VNN1	Pantetheinase	3.22	5.86	4.82	5.14	1.60	1.69	1.45	1.53
VTN	Homeobox protein SEBOX	0.69	0.53	0.66	0.53	0.59	0.41	0.31	0.36
ZBED3	Zinc finger BED domain-containing protein 3	0.59	0.56	0.84	0.66	0.57	0.36	0.33	0.36

\*Ratios from the Loess normalization.

**Table S3. Proteins potentially relevant to fibrotic mechanisms in chronic GVHD**

Protein	Relevant biology	Luminex availability
BMP1	Keloid formation <sup>1</sup>	No
CAST	Skin wound healing and scar formation <sup>2,3</sup>	No
CCL14	M2 macrophage biology, <sup>4</sup> regulation of adhesion molecules and extracellular matrix <sup>5</sup>	<b>Yes</b>
DKK3	Kidney fibrosis, <sup>6</sup> cardiac fibrosis, <sup>7</sup> human keloid, <sup>8</sup> modulator of B cell fate and function <sup>9</sup>	<b>Yes</b>
FGFR1	Pulmonary fibrosis, <sup>10-12</sup> renal fibrosis <sup>13</sup>	No
IL1RAP	Inhibitor of interleukin-1 in collagen-induced arthritis <sup>14,15</sup>	<b>Yes</b>
IL6ST	Fibrosis in the skin, <sup>16</sup> liver <sup>17</sup> and lung <sup>18</sup>	<b>Yes</b>
LAMP2	Immune activation in systemic sclerosis <sup>19</sup>	No
LGALS3BP	Liver fibrosis, <sup>20</sup> monocyte-derived fibrocyte differentiation <sup>21</sup>	<b>Yes</b>
LTBP1	Fibrogenesis <sup>22,23</sup>	No

**Table S4. Linear regression analysis of DKK3 concentrations in patients with chronic GVHD**

**(A) Single regression model**

Factor	N	Fold difference* (95% CI)	P
<b>Cohort</b>			
Discovery	54	1.00 (reference)	
Verification	124	0.77 (0.67-0.87)	<0.001
<b>Duration from HCT to sample draw per year</b>	178	0.93 (0.88-0.98)	0.005
<b>Duration from chronic GVHD to sample draw per year</b>	178	0.93 (0.88-0.98)	0.008

\*Fold difference values represent the anti-log<sub>10</sub> of the regression coefficient.

**(B) Multiple regression model**

Factor	N	Fold difference* (95% CI)	P
<b>Model 1</b>			
<b>Cohort</b>			
Discovery	54	1.00 (reference)	
Verification	124	0.78 (0.66-0.92)	0.003
<b>Duration from HCT to sample draw per year</b>	178	0.99 (0.92-1.06)	0.74
<b>Model 2</b>			
<b>Cohort</b>			
Discovery	54	1.00 (reference)	
Verification	124	0.79 (0.68-0.91)	0.001
<b>Duration from chronic GVHD to sample draw per year</b>	178	0.98 (0.92-1.04)	0.46

\*Fold difference values represent the anti-log<sub>10</sub> of the regression coefficient.

**Table S5. Comparison of GVHD severity and sites between the cohorts**

Characteristic, no (%)	Discovery	Verification	P
<b>NIH global severity</b>			<0.001
Mild	4 (7)	39 (31)	
Moderate	35 (65)	35 (28)	
Severe	15 (15)	50 (40)	
<b>Involved sites</b>			
Skin	38 (70)	74 (60)	0.18
Mouth	39 (72)	58 (47)	0.002
Eye	29 (54)	72 (58)	0.62
Gastrointestinal tract	18 (33)	24 (19)	0.055
Liver	7 (13)	5 (4)	0.047
Lung (BOS)	6 (11)	4 (3)	0.069
Joint/fascia	16 (30)	57 (46)	0.048
Genital	6 (11)	15 (12)	1.0

**Table S6. Linear regression analysis of DKK3 concentrations in patients with chronic GVHD**

Factor	N	Single regression: Unadjusted		Multiple regression: Adjusted	
		Fold difference* (95% CI)	P	Fold difference* (95% CI)	P
<b>Cohort</b>					
Discovery	54	1.00 (reference)		1.00 (reference)	
Verification	124	0.77 (0.67-0.87)	<0.001	0.77 (0.67-0.89)	0.001
<b>NIH global severity</b>					
Mild	43	1.00 (reference)		1.00 (reference)	
Moderate	70	1.26 (1.08-1.47)	0.004	1.15 (0.93-1.41)	0.20
Severe	65	1.20 (1.03-1.40)	0.023	1.19 (0.95-1.48)	0.13
<b>Involved sites</b>					
Skin	112	1.06 (0.93-1.20)	0.39	0.91 (0.77-1.07)	0.23
Mouth	97	1.10 (0.97-1.24)	0.12	1.02 (0.90-1.16)	0.77
Eye	101	1.10 (0.98-1.25)	0.11	1.09 (0.96-1.24)	0.17
Gastrointestinal tract	42	1.07 (0.93-1.24)	0.32	1.00 (0.87-1.16)	0.95
Liver	12	1.06 (0.83-1.36)	0.62	0.99 (0.78-1.27)	0.95
Lung (BOS)	10	1.04 (0.80-1.36)	0.76	0.97 (0.74-1.27)	0.82
Joint/fascia	73	1.05 (0.93-1.18)	0.47	1.05 (0.90-1.23)	0.53
Genital	21	0.93 (0.77-1.13)	0.47	0.89 (0.73-1.07)	0.21

\*Fold difference values represent the anti-log<sub>10</sub> of the regression coefficient.

**Table S7. Sensitivity, specificity, PPV, and NPV associated with chronic GVHD in the verification cohort**

Event	Threshold, $\text{Log}_{10}$ pg/ml	# above threshold	Sensitivity	Specificity	PPV	NPV
<b>Chronic GVHD overall</b>	4.5	181	0.99	0.06	0.68	0.80
	4.6	162	0.96	0.31	0.73	0.79
	4.7	136	0.88	0.56	0.80	0.70
	4.8	101	0.71	0.81	0.88	0.59
	4.9	71	0.55	0.95	0.96	0.51
	5.0	42	0.34	1.00	1.00	0.43
	5.1	14	0.11	1.00	1.00	0.36
	5.2	6	0.05	1.00	1.00	0.64
<b>Moderate to severe chronic GVHD</b>	4.5	181	0.99	0.04	0.46	0.80
	4.6	162	0.95	0.20	0.50	0.83
	4.7	136	0.89	0.41	0.56	0.82
	4.8	101	0.79	0.66	0.66	0.79
	4.9	71	0.62	0.82	0.75	0.72
	5.0	42	0.38	0.90	0.76	0.63
	5.1	14	0.13	0.97	0.79	0.57
	5.2	6	0.05	0.98	0.67	0.55

PPV, positive predictive value; NPV, negative predictive value.

**Table S8. Linear single regression analysis of patient age for DKK3 concentrations in the verification cohort**

Factor	N	Fold difference* (95% CI)	P
Patient age at sample in patients without chronic GVHD, continuous (per decade)	62	1.06 (0.99-1.12)	0.078
Patient age at sample in patients with chronic GVHD, continuous (per decade)	124	1.08 (1.02-1.14)	0.005

\*Fold difference values represent the anti-log<sub>10</sub> of the regression coefficient.

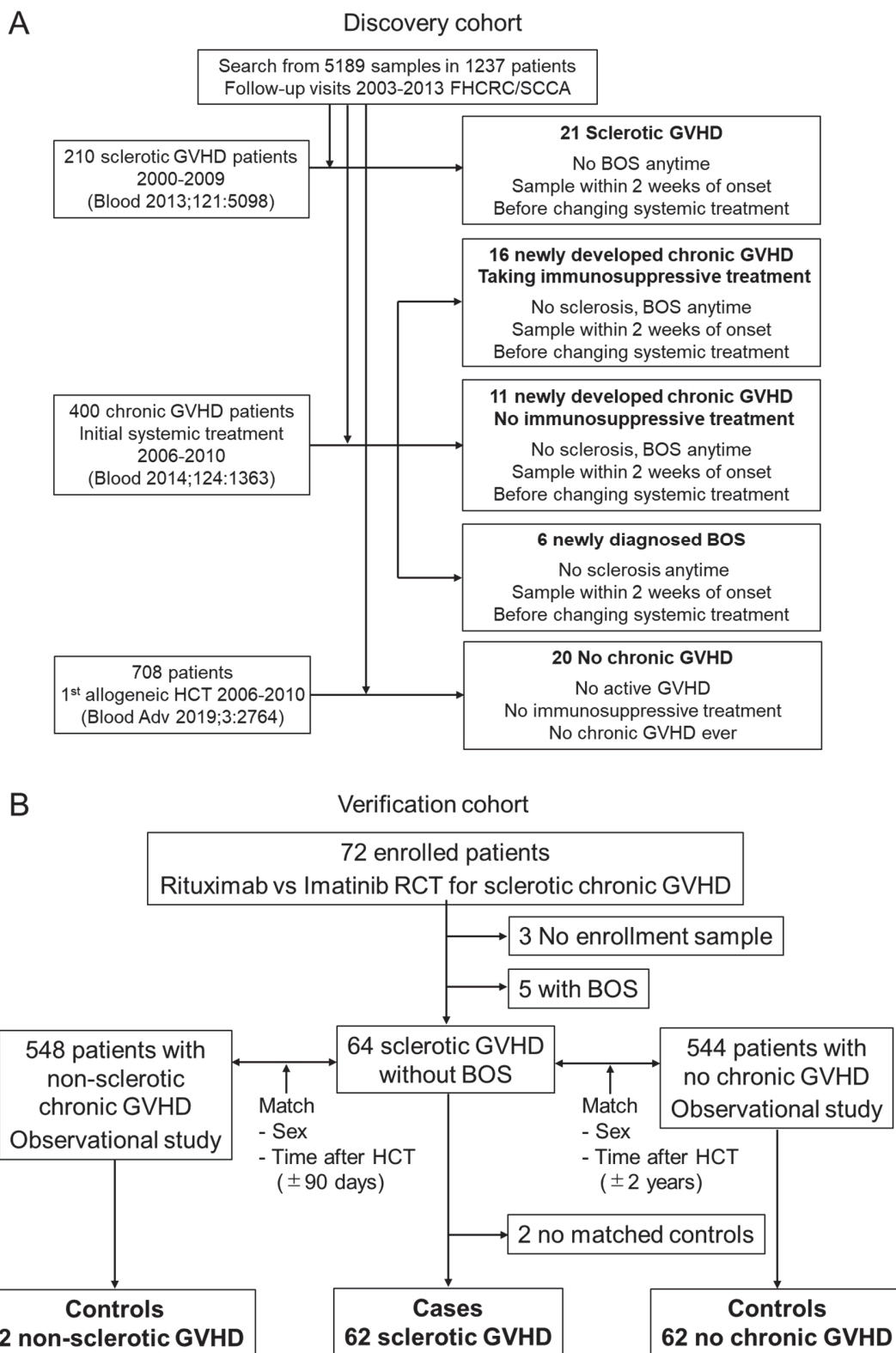


**Figure S1.** CONSORT diagram for (A) discovery cohort and (B) verification cohort.

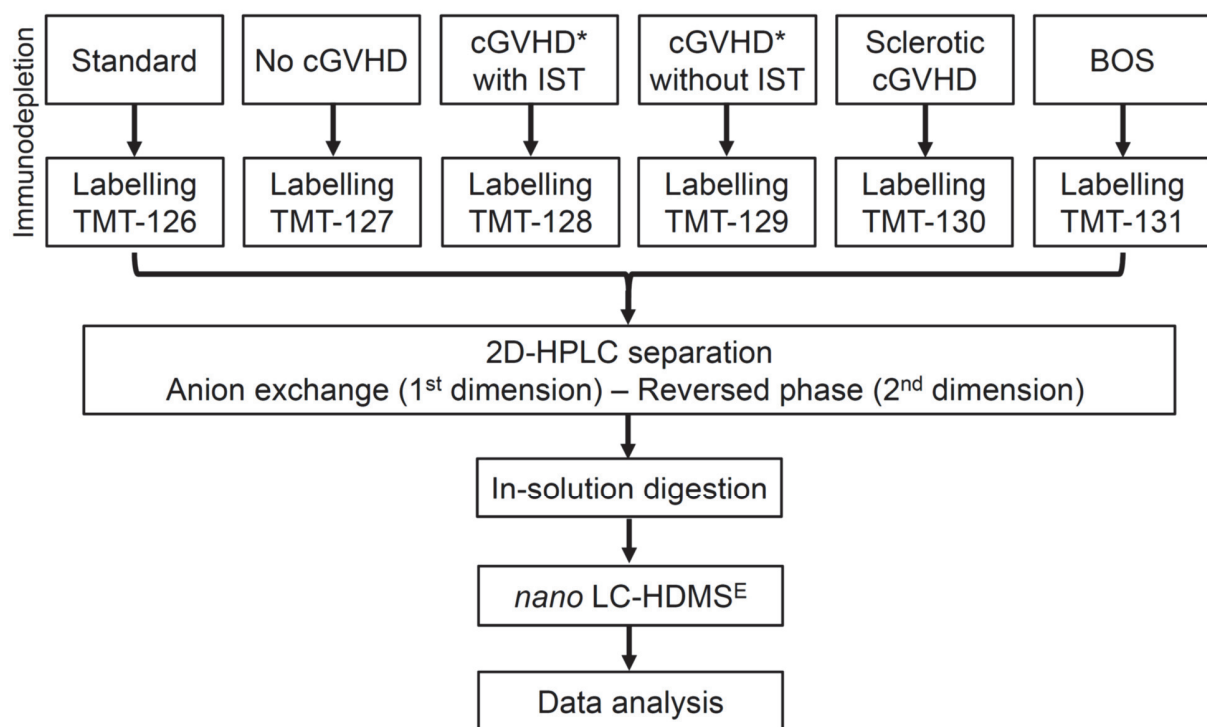


**Figure S2. Quantitative plasma proteomics platform of multiplex mass spectrometry.**

\*Chronic GVHD other than sclerotic chronic GVHD or bronchiolitis obliterans. chronic GVHD, chronic GVHD; IST, immunosuppressive treatment; BOS, bronchiolitis obliterans syndrome; TMT, tandem mass tag; 2D-HPLC, two-dimensional high-performance liquid chromatography; LC-HDMS, liquid chromatography coupled with high-definition mass spectrometry.

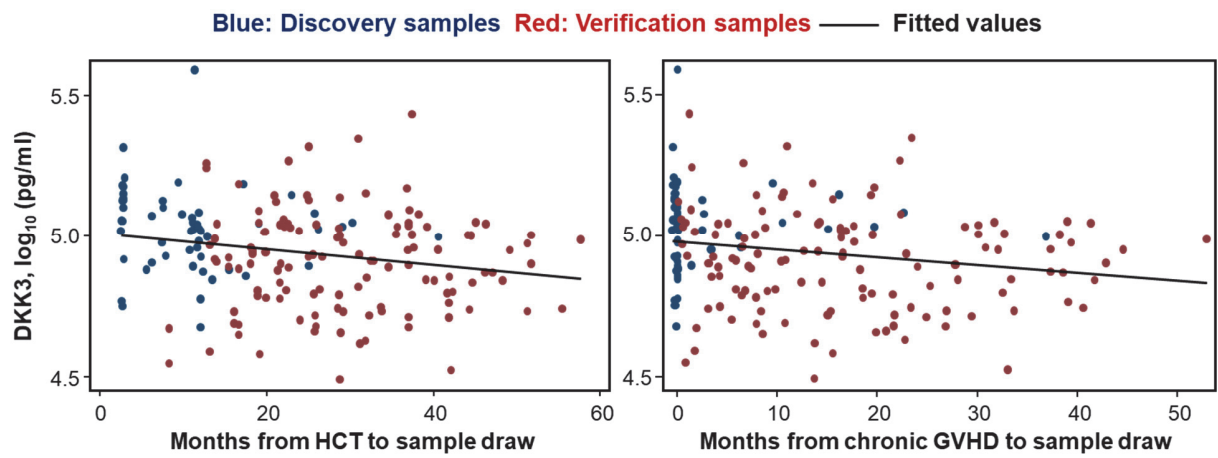


**Figure S3. DKK3 concentrations according to time to sample draw.** Blue dots represent values in discovery samples, and red dots represent values in verification samples. The black line indicates fitted values.

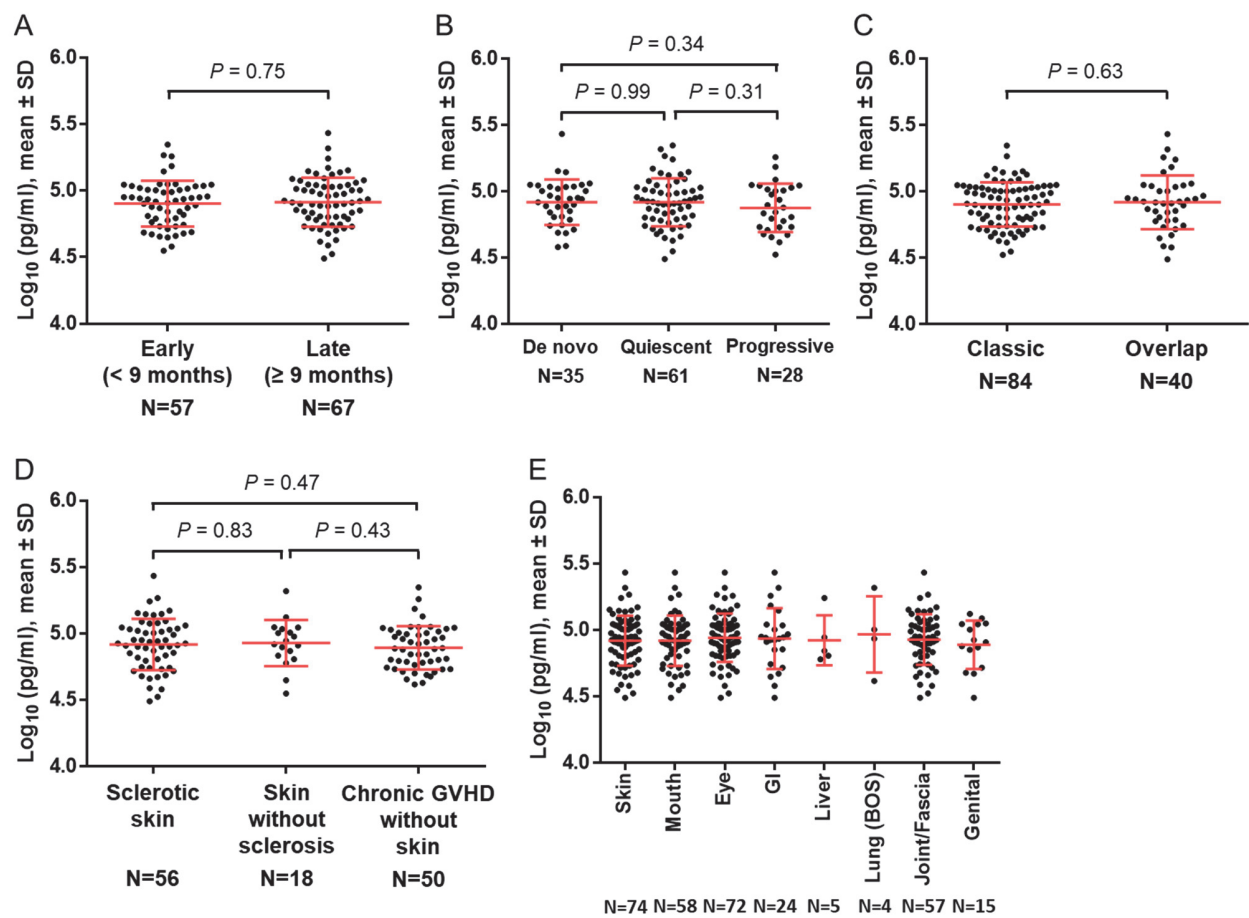


**Figure S4.** DKK3 concentrations according to (A) early (<9 months) vs late onset (≥9 months) chronic GVHD, (B) onset type, (C) chronic GVHD subcategory, (D) skin features, and (E) involved sites in the verification cohort.

**References:**

1. Fuentes-Duculan J, Bonifacio KM, Suarez-Farinas M, et al. Aberrant connective tissue differentiation towards cartilage and bone underlies human keloids in African Americans. *Exp Dermatol*. 2017;26(8):721-727.
2. Nassar D, Letavernier E, Baud L, Aractingi S, Khosrotehrani K. Calpain activity is essential in skin wound healing and contributes to scar formation. *PLoS One*. 2012;7(5):e37084.
3. Lin Z, Zhao J, Nitou D, et al. Loss-of-function mutations in CAST cause peeling skin, leukonychia, acral punctate keratoses, cheilitis, and knuckle pads. *Am J Hum Genet*. 2015;96(3):440-447.
4. Jaguin M, Houlbert N, Fardel O, Lecureur V. Polarization profiles of human M-CSF-generated macrophages and comparison of M1-markers in classically activated macrophages from GM-CSF and M-CSF origin. *Cell Immunol*. 2013;281(1):51-61.
5. Hannan NJ, Salamonsen LA. CX3CL1 and CCL14 regulate extracellular matrix and adhesion molecules in the trophoblast: potential roles in human embryo implantation. *Biol Reprod*. 2008;79(1):58-65.
6. Federico G, Meister M, Mathow D, et al. Tubular Dickkopf-3 promotes the development of renal atrophy and fibrosis. *JCI Insight*. 2016;1(1):e84916.
7. Zhai CG, Xu YY, Tie YY, et al. DKK3 overexpression attenuates cardiac hypertrophy and fibrosis in an angiotensin-perfused animal model by regulating the ADAM17/ACE2 and GSK-3beta/beta-catenin pathways. *J Mol Cell Cardiol*. 2018;114:243-252.
8. Li Y, Liu H, Liang Y, Peng P, Ma X, Zhang X. DKK3 regulates cell proliferation, apoptosis and collagen synthesis in keloid fibroblasts via TGF-beta1/Smad signaling pathway. *Biomed Pharmacother*. 2017;91:174-180.
9. Ludwig J, Federico G, Prokosch S, et al. Dickkopf-3 acts as a modulator of B cell fate and function. *J Immunol*. 2015;194(6):2624-2634.
10. Shimbori C, Bellaye PS, Xia J, et al. Fibroblast growth factor-1 attenuates TGF-beta1-induced lung fibrosis. *J Pathol*. 2016;240(2):197-210.
11. Guzy RD, Li L, Smith C, et al. Pulmonary fibrosis requires cell-autonomous mesenchymal fibroblast growth factor (FGF) signaling. *J Biol Chem*. 2017;292(25):10364-10378.
12. MacKenzie B, Korfei M, Henneke I, et al. Increased FGF1-FGFRc expression in idiopathic pulmonary fibrosis. *Respir Res*. 2015;16:83.
13. Liu F, Wang L, Qi H, et al. Nintedanib, a triple tyrosine kinase inhibitor, attenuates renal fibrosis in chronic kidney disease. *Clin Sci (Lond)*. 2017;131(16):2125-2143.
14. Smeets RL, van de Loo FA, Joosten LA, et al. Effectiveness of the soluble form of the interleukin-1 receptor accessory protein as an inhibitor of interleukin-1 in collagen-induced arthritis. *Arthritis Rheum*. 2003;48(10):2949-2958.

15. Smeets RL, Joosten LA, Arntz OJ, et al. Soluble interleukin-1 receptor accessory protein ameliorates collagen-induced arthritis by a different mode of action from that of interleukin-1 receptor antagonist. *Arthritis Rheum.* 2005;52(7):2202-2211.
16. Hasegawa M, Sato S, Fujimoto M, Ihn H, Kikuchi K, Takehara K. Serum levels of interleukin 6 (IL-6), oncostatin M, soluble IL-6 receptor, and soluble gp130 in patients with systemic sclerosis. *J Rheumatol.* 1998;25(2):308-313.
17. Streetz KL, Tacke F, Leifeld L, et al. Interleukin 6/gp130-dependent pathways are protective during chronic liver diseases. *Hepatology.* 2003;38(1):218-229.
18. Moodley YP, Scaffidi AK, Misso NL, et al. Fibroblasts isolated from normal lungs and those with idiopathic pulmonary fibrosis differ in interleukin-6/gp130-mediated cell signaling and proliferation. *Am J Pathol.* 2003;163(1):345-354.
19. Holcombe RF, Baethge BA, Stewart RM, et al. Cell surface expression of lysosome-associated membrane proteins (LAMPs) in scleroderma: relationship of lamp2 to disease duration, anti-Sc170 antibodies, serum interleukin-8, and soluble interleukin-2 receptor levels. *Clin Immunol Immunopathol.* 1993;67(1):31-39.
20. Cheung KJ, Libbrecht L, Tilleman K, Deforce D, Colle I, Van Vlierberghe H. Galectin-3-binding protein: a serological and histological assessment in accordance with hepatitis C-related liver fibrosis. *Eur J Gastroenterol Hepatol.* 2010;22(9):1066-1073.
21. White MJ, Roife D, Gomer RH. Galectin-3 Binding Protein Secreted by Breast Cancer Cells Inhibits Monocyte-Derived Fibrocyte Differentiation. *J Immunol.* 2015;195(4):1858-1867.
22. Kim HS, Yoon YM, Meang MK, et al. Reversion of in vivo fibrogenesis by novel chromone scaffolds. *EBioMedicine.* 2019;39:484-496.
23. Caja L, Dituri F, Mancarella S, et al. TGF-beta and the Tissue Microenvironment: Relevance in Fibrosis and Cancer. *Int J Mol Sci.* 2018;19(5).